

See discussions, stats, and author profiles for this publication at: <https://www.researchgate.net/publication/41410786>

Synthesis of a Triptycene-Derived Bisparaphenylene-34-crown-10 and Its Complexation with Both Paraquat and Cyclobis(paraquat-p-phenylene)

ARTICLE *in* THE JOURNAL OF ORGANIC CHEMISTRY · FEBRUARY 2010

Impact Factor: 4.72 · DOI: 10.1021/jo902571n · Source: PubMed

CITATIONS

25

READS

23

5 AUTHORS, INCLUDING:



Yi Jiang

Chinese Academy of Sciences

26 PUBLICATIONS 321 CITATIONS

SEE PROFILE



Jing Cao

18 PUBLICATIONS 205 CITATIONS

SEE PROFILE



Jun-Feng Xiang

Chinese Academy of Sciences

185 PUBLICATIONS 2,878 CITATIONS

SEE PROFILE



Chuan-Feng Chen

Chinese Academy of Sciences

155 PUBLICATIONS 4,128 CITATIONS

SEE PROFILE

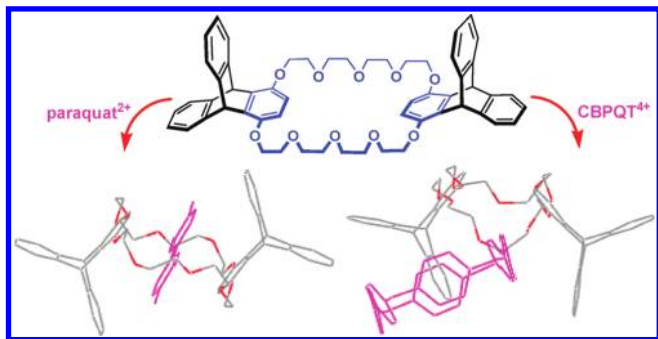
Synthesis of a Triptycene-Derived Bisparaphenylene-34-crown-10 and Its Complexation with Both Paraquat and Cyclobis(paraquat-*p*-phenylene)

Yi Jiang,^{†,‡} Jing Cao,^{†,‡} Jian-Min Zhao,^{†,‡} Jun-Feng Xiang,[†] and Chuan-Feng Chen^{*,†}

[†]Beijing National Laboratory for Molecular Sciences, CAS Key Laboratory of Molecular Recognition and Function, Institute of Chemistry, Chinese Academy of Sciences, Beijing 100190, China, and [‡]Graduate School, Chinese Academy of Sciences, Beijing 100049, China

cchen@iccas.ac.cn

Received December 4, 2009



A novel triptycene-derived bisparaphenylene-34-crown-10 (**1**) has been synthesized, and shown to form 1:1 stable complexes with both the paraquat **G1**·**2PF₆** and the cyclobis(paraquat-*p*-phenylene) **G2**·**4PF₆** in different complexation modes in solution and solid state. Moreover, it was found that both the complexes **1**·**G1**·**2PF₆** and **1**·**G2**·**4PF₆** were formed by charge transfer interactions, and did not dissociate upon the first one-electron reduction process of the bipyridinium ring.

Host–guest chemistry¹ has attracted much attention since Pedersen first reported² the synthesis and cation-complexing characteristics of crown ethers. As a member of crown ethers,³ the bisparaphenylene-34-crown-10 (BPP34C10)⁴ has found wide applications in host–guest chemistry, especially

in the formation of a variety of interlocked assemblies.⁵ On the other hand, cyclobis(paraquat-*p*-phenylene) (CBPQT)^{6a} with considerable binding affinity for π -donor systems has been extensively utilized by Stoddart's group and others in the construction of various interlocked structures.^{6b,c} However, until recently, only two examples⁷ of the CBPQT⁴⁺ ring acting as a guest in the formation of the complexes were reported.

During the past several years, we have proven that the triptycene with unique 3D rigid structure could be utilized as a useful building block for the synthesis of novel macrocyclic hosts with specific structures and properties.⁸ As part of our continuing work, we herein report the synthesis and binding properties of a novel triptycene-derived bisparaphenylene-34-crown-10 (**1**, Figure 1). Due to its electron-rich cavity, **1** can form stable complexes with both the paraquat **G1**·**2PF₆** and the cyclobis(paraquat-*p*-phenylene) **G2**·**4PF₆** in different complexation modes in solution and solid state. Especially, it is interestingly found that both **1** and **G2**·**4PF₆** act as not only the host but also the guest in complex **1**·**G2**·**4PF₆**. Moreover, it was also found that both complexes **1**·**G1**·**2PF₆** and **1**·**G2**·**4PF₆** were formed by charge transfer interactions, and did not dissociate upon the first one-electron reduction process of the bipyridinium ring.

The synthesis of compound **1** is outlined in Scheme 1. First, triptycene derivative **3** was synthesized in 69% yield by the reaction of compound **5**⁹ with diethylene glycol mono-*p*-toluenesulfonate **4** in CH₃CN in the presence of K₂CO₃. By treatment of compound **3** with TsCl in CH₂Cl₂ in the presence of Et₃N, compound **2** was obtained in 77% yield. Finally, the target molecule **1** was produced in 17% yield by the reaction of **2** and **3** in THF in the presence of NaH. All new compounds were confirmed by ¹H NMR, ¹³C NMR, MS-TOF spectra, and elemental analysis.¹⁰

(5) (a) Ashton, P. R.; Ballardini, R.; Balzani, V.; Credi, A.; Gandolfi, M. T.; Menzer, S.; Pérez-García, L.; Prodi, L.; Stoddart, J. F.; Venturi, J. M.; White, A. J. P.; Williams, D. J. *J. Am. Chem. Soc.* **1995**, *117*, 11171–11197. (b) Asakawa, M.; Brown, C. L.; Menzer, S.; Raymo, F. M.; Stoddart, J. F.; Williams, D. J. *J. Am. Chem. Soc.* **1997**, *119*, 2614–2627. (c) Liu, Y.; Klivansky, L. M.; Khan, S. I.; Zhang, X. *Org. Lett.* **2007**, *9*, 2577–2580.

(6) (a) Odell, B.; Reddington, M. V.; Slawin, A. M. Z.; Spencer, N.; Stoddart, J. F.; Williams, D. J. *Angew. Chem., Int. Ed. Engl.* **1988**, *27*, 1547–1550. (b) Flood, A. H.; Stoddart, J. F.; Steuerman, D. W.; Heath, J. R. *Science* **2004**, *306*, 2055–2056. (c) Deng, W.-Q.; Flood, A. H.; Stoddart, J. F.; Goddard, W. A. III *J. Am. Chem. Soc.* **2005**, *127*, 15994–15995. (d) Nygaard, S.; Laursen, B. W.; Flood, A. H.; Hansen, C. N.; Jeppesen, J. O. *Chem. Commun.* **2006**, 144–146. (e) Liu, Y.; Bonvallet, P. A.; Vignon, S. A.; Khan, S. I.; Stoddart, J. F. *Angew. Chem., Int. Ed.* **2005**, *44*, 3050–3055. (f) Liu, Y.; Flood, A. H.; Bonvallet, P. A.; Vignon, S. A.; Northrop, B. H.; Tseng, H.-R.; Jeppesen, J. O.; Huang, T. J.; Brough, B.; Baller, M.; Magonov, S.; Solares, S. D.; Goddard, W. A.; Ho, C.-M.; Stoddart, J. F. *J. Am. Chem. Soc.* **2005**, *127*, 9745–9759.

(7) (a) Cao, J.; Jiang, Y.; Zhao, J.-M.; Chen, C.-F. *Chem. Commun.* **2009**, 1987–1989. (b) Jiang, J.; MacLachlan, M. J. *Chem. Commun.* **2009**, 5695–5697.

(8) (a) Zhu, X.-Z.; Chen, C.-F. *J. Am. Chem. Soc.* **2005**, *127*, 13158–13159. (b) Zong, Q.-S.; Chen, C.-F. *Org. Lett.* **2006**, *8*, 211–214. (c) Han, T.; Chen, C.-F. *Org. Lett.* **2006**, *8*, 1069–1072. (d) Zhu, X.-Z.; Chen, C.-F. *Chem.—Eur. J.* **2006**, *12*, 5603–5609. (e) Peng, X.-X.; Lu, H.-Y.; Han, T.; Chen, C.-F. *Org. Lett.* **2007**, *9*, 895–898. (f) Xue, M.; Chen, C.-F. *Chem. Commun.* **2008**, 6128–6130. (g) Xue, M.; Chen, C.-F. *Org. Lett.* **2009**, *11*, 5294–5297. (h) Tian, X.-H.; Hao, X.; Liang, T.-L.; Chen, C.-F. *Chem. Commun.* **2009**, 6771–6773.

(9) Bartlett, P. D.; Ryan, M. J.; Cohen, S. *J. Am. Chem. Soc.* **1942**, *64*, 2649–2653.

(10) See the Supporting Information

(1) (a) Cram, D. J.; Cram, J. M. *Container Molecules and Their Guests*; Royal Society of Chemistry: Cambridge, UK, 1994. (b) Lehn, J.-M. *Supramolecular Chemistry*; VCH Publishers: New York, 1995.

(2) Pedersen, C. J. *J. Am. Chem. Soc.* **1967**, *89*, 7017–7036.

(3) (a) Badjic, J. D.; Balzani, V.; Credi, A.; Silvi, S.; Stoddart, J. F. *Science* **2004**, *303*, 1845–1849. (b) Badjic, J. D.; Cantrill, S. J.; Stoddart, J. F. *J. Am. Chem. Soc.* **2004**, *126*, 2288–2289. (c) Huang, F.; Fronczek, F. R.; Gibson, H. W. *Chem. Commun.* **2003**, 1480–1481. (d) Long, B.; Nikitin, K.; Fitzmaurice, D. *J. Am. Chem. Soc.* **2003**, *125*, 15490–15498.

(4) Allwood, B. L.; Spencer, N.; Shahriari-Zavareh, H.; Stoddart, J. F.; Williams, D. J. *J. Chem. Soc., Chem. Commun.* **1987**, 1064–1066.

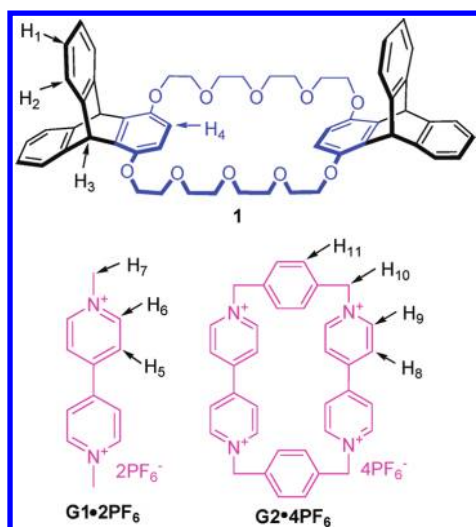
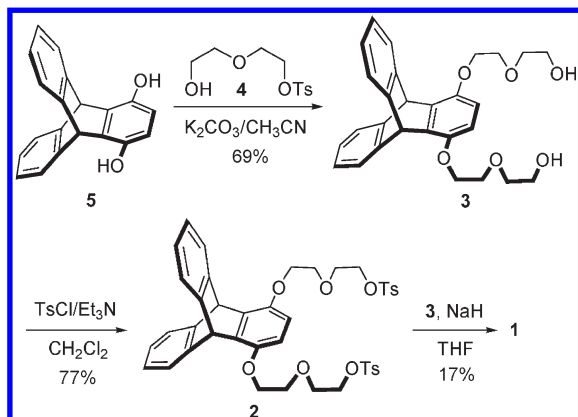


FIGURE 1. Structures and the proton designations of triptycene-derived BPP34C10 **1**, the paraquat **G1·2PF₆**, and the CBPQT⁴⁺ salt **G2·4PF₆**.

SCHEME 1. Synthesis of the Triptycene-Derived BPP34C10 **1**



We first investigated the complexation between **1** and **G1·2PF₆** in solution. Consequently, when **1** and **G1·2PF₆** (1 mM each) were mixed in chloroform and acetonitrile (3:1), a color change from colorless to yellow was immediately shown, which could be due to the charge transfer interaction between the electron-rich aromatic rings of **1** and the electron-poor bipyridinium ring of **G1·2PF₆**.¹⁰ The ¹H NMR spectrum of a 1:1 mixture of **1** and **G1·2PF₆** in CDCl₃ and CD₃CN (3:1) also showed a great difference from those for **1** and **G1·2PF₆**.¹⁰ Especially, it was found that the protons H₅ and H₆ of the pyridinium ring shifted significantly upfield, which might be due to the strong shielding affect of the aromatic rings of **1**. These observations suggested that a new complex **1·G1·2PF₆** was formed. The ¹H NMR spectroscopic titrations further afforded a quantitative estimate for the complexation between **1** and **G1·2PF₆** by monitoring the changes of the chemical shift of the proton H₆ of **G1·2PF₆**. The results showed that a 1:1 complex between **1** and **G1·2PF₆** was formed by a mole ratio plot. Accordingly, the apparent association constant $K_{a,exp}$ was calculated to be $2100(\pm 100) \text{ M}^{-1}$ by the Scatchard plot.^{8c,11}

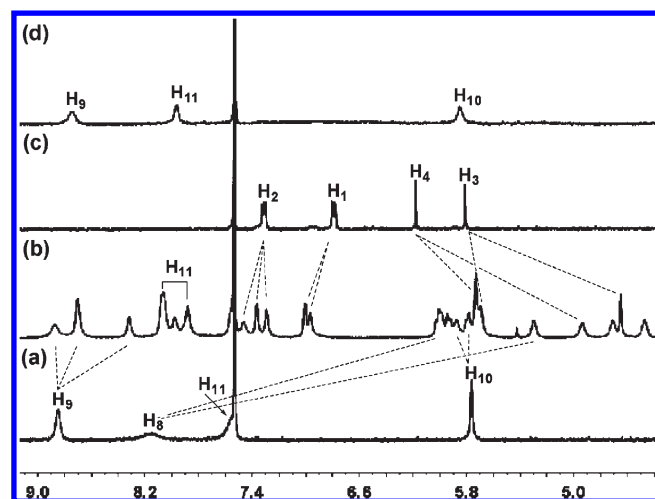


FIGURE 2. Partial ¹H NMR spectra (600 MHz, CDCl₃:CD₃CN = 1:2) of (a) **G2·4PF₆** at 298 K, (b) **1** and 1.0 equiv of **G2·4PF₆** at 238 K, (c) **1** at 298 K, (d) **1** and 1.0 equiv of **G2·4PF₆** at 298 K. [**1**]₀ = 1 mM.

Similar to the case of **1** and **G1·2PF₆**, mixing **1** and the CBPQT⁴⁺ ring (1 mM each) in chloroform and acetonitrile (1:2) also showed a swift color change from pale yellow to a light red-brown, which might be due to the charge transfer between the electron-rich aromatic rings of **1** and the bipyridinium rings of **G2·4PF₆**.¹⁰ In the ¹H NMR spectrum of a mixture of **1** and **G2·4PF₆** in 1:2 CDCl₃ and CD₃CN at 298 K (Figure 2d), it was found that the H₉ proton signal of **G2·4PF₆** shifted upfield, which might be due to the strong shielding effect of the aromatic rings in **1**. Meanwhile, an obvious change in the chemical shift of the proton H₁₁ ($\Delta\delta = 0.43 \text{ ppm}$) of **G2·4PF₆** was also observed. Except for H₉ and H₁₁, other aromatic proton signals almost disappeared at 298 K, which might be due to the effect of the swift exchange process of the complex.¹² To further study the complexation between **1** and **G2·4PF₆** in solution, the ¹H NMR experiments of the complex in 1:2 CDCl₃ and CD₃CN at low temperatures were then carried out.¹⁰ The results showed that with lowering of the temperature, the aromatic proton signals broadened gradually, and then split into complex ones at 238 K (Figure 2b), which indicated that the exchange of the complex slowed down at low temperatures, and complex **1·G2·4PF₆** showed a highly asymmetric structure in solution. Furthermore, a quantitative estimate for the complexation between **1** and **G2·4PF₆** was also obtained by monitoring the changes of the chemical shift of the proton H₁₁ of **G2·4PF₆** at 298 K. The results showed that **1** and **G2·4PF₆** formed a 1:1 complex **1·G2·4PF₆**. Accordingly, the apparent association constant was calculated to be $1.93(\pm 0.07) \times 10^4 \text{ M}^{-1}$ by the Scatchard plot.^{8c,11}

Formation of the 1:1 stable complexes **1·G1·2PF₆** and **1·G2·4PF₆** was also evidenced by the electrospray ionization mass spectra.¹⁰ As a result, the strong peaks at m/z 537.38 for $[\mathbf{1} \cdot \mathbf{G1} \cdot 2\text{PF}_6 - 2\text{PF}_6]^{2+}$, and 518.13 for $[\mathbf{1} \cdot \mathbf{G2} \cdot 4\text{PF}_6 - 3\text{PF}_6]^{3+}$ were observed, respectively.

Further support for formation of complexes **1·G1·2PF₆** and **1·G2·4PF₆** came from their X-ray diffraction results. As

(11) Connors, K. A. *Binding Constants*; J. Wiley and Sons: New York, 1987.

(12) Sanders, L. K. M.; Hunter, B. K. *Modern NMR Spectroscopy*; Oxford University Press: New York, 1987.

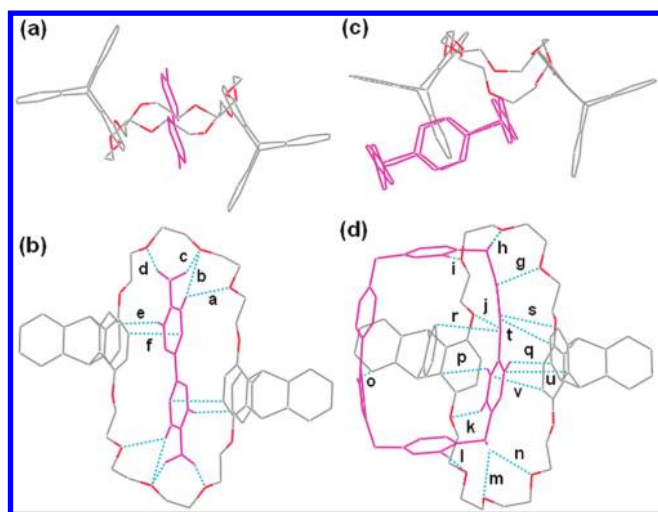


FIGURE 3. Views of the crystal structures of (a, b) $1 \cdot \text{G1} \cdot 2\text{PF}_6$, and (c, d) $1 \cdot \text{G2} \cdot 4\text{PF}_6$. Blue lines denote the noncovalent interactions between the host and the guest. The C–H \cdots O hydrogen bond distances (Å) for $1 \cdot \text{G1} \cdot 2\text{PF}_6$: $a = 2.60$; $b = 2.66$; $c = 2.70$; $d = 2.37$. The C–H \cdots O hydrogen bond distances (Å) for $1 \cdot \text{G2} \cdot 4\text{PF}_6$: $g = 2.69$; $h = 2.20$; $i = 2.40$; $j = 2.70$; $k = 2.55$; $l = 2.47$; $m = 2.54$; $n = 2.57$. Solvent molecules, PF_6^- counterions, and hydrogen atoms not involved in the noncovalent interactions are omitted for clarity.

shown in Figure 3, it was found that **1** could adopt different conformations to bind $\text{G1} \cdot 2\text{PF}_6$ or $\text{G2} \cdot 4\text{PF}_6$ in the solid state. In the complex $1 \cdot \text{G1} \cdot 2\text{PF}_6$ (Figure 3a), the two triptycene moieties in **1** were positioned in the different sides of the crown ether, in which every benzene ring of one triptycene paralleled with one benzene ring of another triptycene. Meanwhile, the paraquat ring was positioned in about a crystallographic center of symmetry, and formed a pseudosandwiched structure with two triptycene moieties. In the crystal structure of $1 \cdot \text{G2} \cdot 4\text{PF}_6$ (Figure 3c), the two triptycene moieties in **1** were positioned in the same side of the crown ether to form a tweezer-like cavity, which is completely different from that of $1 \cdot \text{G1} \cdot 2\text{PF}_6$. Moreover, it was interestingly found that in $1 \cdot \text{G2} \cdot 4\text{PF}_6$ not only is one of the 4,4'-bipyridinium rings of $\text{G2} \cdot 4\text{PF}_6$ included in the cavity of the tweezer-like **1**, but also one benzene ring of the triptycene moieties was positioned inside the cavity of $\text{G2} \cdot 4\text{PF}_6$. These results not only explained the reason for the complexed ^1H NMR spectra of $1 \cdot \text{G2} \cdot 4\text{PF}_6$ at low temperatures, but also indicated that **1** and $\text{G2} \cdot 4\text{PF}_6$ formed a pseudoternary complex, in which the two receptors acted as both the host and the guest.

As shown in Figure 3b, it was further found that there existed multiple C–H \cdots O hydrogen bonding interactions between the polyether oxygen atoms of **1** and both the aromatic protons and the methyl protons in $\text{G1} \cdot 2\text{PF}_6$. Moreover, a pair of π – π stacking interactions with a distance of 3.27 Å (f) between the paraquat ring and the benzene rings of the triptycene moieties in **1**, and a pair of C–H \cdots π interactions between the aromatic protons in $\text{G1} \cdot 2\text{PF}_6$ and the benzene rings of the triptycene moieties with a distance of 2.71 Å (e) were observed. These multiple noncovalent interactions played an important role in the formation of the stable complex $1 \cdot \text{G1} \cdot 2\text{PF}_6$. Similarly, in complex $1 \cdot \text{G2} \cdot 4\text{PF}_6$ there also existed multiple C–H \cdots O

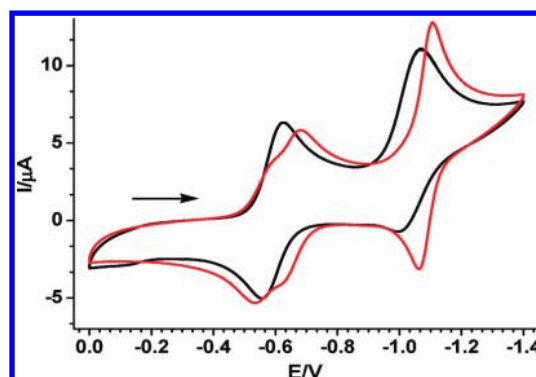


FIGURE 4. CV curves for a solution of G2^{4+} (0.5×10^{-3} M) in $\text{CH}_3\text{CN}:\text{CHCl}_3$ (2:1, v/v) with $(\text{NBu}_4)\text{PF}_6$ (0.1 M) as the supporting electrolyte in the absence (black line) and the presence (red line) of **1** (1.0×10^{-3} M). Working electrode: Pt. Scan rate: 0.1 V s^{-1} .

hydrogen bonding interactions between the polyether oxygen atoms of **1** and the aromatic protons and the methylene protons in $\text{G2} \cdot 4\text{PF}_6$. Moreover, C–H \cdots π interactions between the aromatic protons in $\text{G2} \cdot 4\text{PF}_6$ and the benzene rings of the triptycene moieties with distances of 2.66 (o), 2.81 (p), 2.84 (q), and 2.89 Å (s), and π – π stacking interactions between the benzene rings of the triptycenes in **1** and the bipyridinium rings in $\text{G2} \cdot 4\text{PF}_6$ with distances of 3.39 (r), 3.34 (s), 3.36 (u), and 3.34 Å (v) were also observed (Figure 3d). In addition, due to the unique structural property of the triptycene moieties, the adjacent molecules of **1** could further be connected with each other by complexation with another 4,4'-bipyridinium ring of $\text{G2} \cdot 4\text{PF}_6$, which resulted in a 1D supramolecular polymer in the solid state.¹⁰

Since both $\text{G1} \cdot 2\text{PF}_6$ and $\text{G2} \cdot 4\text{PF}_6$ are well-known organic redox-active molecules, their electrochemical behaviors in the absence and presence of **1** were also studied. It was known that the G1^{2+} showed two one-electron reduction processes¹³ corresponding to the successive reduction of the 4,4'-bipyridinium core. Upon the addition of **1** to the 2:1 CH_3CN and CHCl_3 solution of $\text{G1} \cdot 2\text{PF}_6$, both the cathodic and anodic peaks of the first one-electron reduction process moved to the more negative values, and the peaks corresponding to the second one-electron reduction process also slightly moved to the more negative values,¹⁰ which suggested that complex $1 \cdot \text{G1} \cdot 2\text{PF}_6$ formed, and it did not dissociate upon the first one-electron reduction process of the bipyridinium ring. Similar to $\text{G1} \cdot 2\text{PF}_6$, $\text{G2} \cdot 4\text{PF}_6$ also showed two reversible two-electron redox processes with the half-wave potential values at -0.591 and $-1.031 \text{ V vs Ag/AgNO}_3$, respectively.¹⁴ As shown in Figure 4, the CV patterns for reduction of the G2^{4+} were remarkably affected upon the addition of **1**. The first reduction process of $\text{G2} \cdot 4\text{PF}_6$ displayed a splitting of 87 mV, and also the split peaks moved to less negative potential, which was considered the result of the mixing of the HOMO of the electron-donor

(13) (a) Balzani, V.; Ceroni, P.; Giansante, C.; Vicinelli, V.; Klärner, F.; Verhaelen, C.; Vögtle, F.; Hahn, U. *Angew. Chem., Int. Ed.* **2005**, *44*, 4574–4578. (b) Balzani, V.; Bandmann, H.; Ceroni, P.; Giansante, C.; Hahn, U.; Klärner, F.; Müller, U.; Müller, W. M.; Verhaelen, C.; Vicinelli, V.; Vögtle, F. *J. Am. Chem. Soc.* **2006**, *128*, 637–648.

(14) Anelli, P. L.; Ashton, P. R.; Ballardini, R.; Balzani, V.; Delgado, M.; Gandolfi, M. T.; Goodnow, T. T.; Kaifer, A. E.; Philp, D.; Pietraszkiewicz, M.; Prodi, L.; Reddington, M. V.; Slawin, A. M. Z.; Spencer, N.; Stoddart, J. F.; Vicent, C.; Williams, D. J. *J. Am. Chem. Soc.* **1992**, *114*, 193–218.

(1) and the LUMO of the electron-acceptor ($\mathbf{G2}^{4+}$) through charge transfer interaction, whereas the peak corresponding to the second reduction process shifted to the more negative potential. These behaviors showed that the formation of the adduct was caused by a CT interaction, and the adduct did not dissociate upon the first one-electron reduction of $\mathbf{G2}^{4+}$.¹⁵

In summary, we have synthesized a novel triptycene-derived bisparaphenylene-34-crown-10 (**1**), and demonstrated that it could form 1:1 stable complexes with both paraquat $\mathbf{G1} \cdot 2\mathbf{PF}_6$ and cyclobis(paraquat-*p*-phenylene) $\mathbf{G2} \cdot 4\mathbf{PF}_6$ in different modes in solution and solid state. Especially, it was found that **1** and $\mathbf{G2} \cdot 4\mathbf{PF}_6$ could form a pseudoternary complex, in which the two molecules acted as not only the host but also the guest. Moreover, we also found that both complexes $\mathbf{1} \cdot \mathbf{G1} \cdot 2\mathbf{PF}_6$ and $\mathbf{1} \cdot \mathbf{G2} \cdot 4\mathbf{PF}_6$ were formed by charge transfer interactions, and did not dissociate upon the first one-electron reduction process of the bipyridinium ring.

Experimental Section

Compound 3. A mixture of **4** (2.49 g, 9.6 mmol), **5** (1.37 g, 4.8 mmol), and K_2CO_3 (2.76 g, 20 mmol) in dried CH_3CN (150 mL) was refluxed under N_2 atmosphere over 24 h. The reaction mixture was cooled to room temperature, and then filtered. The filtrate was concentrated to give a residue, which was purified by silica gel column chromatography (eluant: 100:1 CH_2Cl_2 /methanol) to afford **3** (1.535 g, 69%) as a colorless solid. Mp: 145–146 °C. ^1H NMR (300 MHz, CDCl_3): δ 7.38–7.40 (m, 4H), 6.95–6.98 (m, 4H), 6.50 (s, 2H), 5.88 (s, 2H), 4.07–4.1 (m, 4H), 3.87–3.91 (m, 4H), 3.78–3.82 (m, 4H), 3.72–3.74 (m, 4H), 2.26 (s, 2H). ^{13}C NMR (75 MHz, CDCl_3): δ 148.5, 145.6, 136.2, 125.0, 123.8, 111.2, 72.5, 69.9, 69.4, 61.9, 47.5. MALDI-TOF MS: m/z 485.4 $[\text{M} + \text{Na}]^+$, 501.4 $[\text{M} + \text{K}]^+$. Anal. Calcd for $\text{C}_{28}\text{H}_{30}\text{O}_6$: C, 72.71; H, 6.54. Found: C, 72.50; H, 6.41.

Compound 2. To a solution of **3** (0.45 g, 0.97 mmol) in dried dichloromethane (50 mL) in an ice bath was added TsCl (0.48 g, 2.5 mmol), Et_3N (0.7 mL, 5 mmol), and DMAP (15 mg). After

being refluxed overnight, the filtrate was removed in vacuo. The residue was purified by silica gel column chromatography (eluant: 200:1 CH_2Cl_2 /methanol) to afford **2** (575 mg, 77%) as a pale yellow solid. Mp: 146–147 °C. ^1H NMR (300 MHz, CDCl_3): δ 7.80 (d, J = 7.80 Hz, 4H), 7.34–7.37 (m, 4H), 7.25 (d, J = 7.25 Hz, 4H), 6.94–6.96 (m, 4H), 6.47 (s, 2H), 5.84 (s, 2H), 4.22–4.26 (m, 4H), 3.99–4.02 (m, 4H), 3.80–3.84 (m, 4H), 2.35 (s, 6H). ^{13}C NMR (75 MHz, CDCl_3): δ 148.4, 145.6, 144.8, 136.3, 133.1, 129.8, 128.0, 125.0, 123.8, 111.4, 70.1, 69.5, 69.3, 68.9, 47.4, 21.6. MALDI-TOF MS: m/z 793.6 $[\text{M} + \text{Na}]^+$, 809.6 $[\text{M} + \text{K}]^+$. Anal. Calcd for $\text{C}_{42}\text{H}_{42}\text{O}_{10}\text{S}_2$: C, 65.44; H, 5.49. Found: C, 65.65; H, 5.29.

Compound 1. A solution of **2** (333 mg, 0.43 mmol) and **3** (200 mg, 0.43 mmol) in THF (50 mL) was added dropwise to a suspension of NaH (200 mg, 8.3 mmol) in THF (50 mL) at 80 °C under N_2 atmosphere. The reaction was continued for another 48 h. The reaction mixture was cooled to room temperature, water was added, and then the solution was filtered. The filtrate was concentrated under reduced pressure, and the residue was purified by silica gel column chromatography (eluant: 100:1 CH_2Cl_2 /methanol) to afford **1** (65 mg, 17%). Mp: > 300 °C. ^1H NMR (300 MHz, CDCl_3): δ 7.30–7.32 (m, 8H), 6.79–6.82 (m, 8H), 6.16 (s, 4H), 5.81 (s, 4H), 3.84–3.87 (m, 8H), 3.72–3.77 (m, 24H). ^{13}C NMR (75 MHz, CDCl_3): δ 148.3, 145.6, 135.8, 124.8, 123.7, 111.4, 77.4, 77.2, 77.0, 76.6, 71.0, 70.9, 69.8, 69.4, 47.4. MALDI-TOF MS: m/z 911.8 $[\text{M} + \text{Na}]^+$, 927.8 $[\text{M} + \text{K}]^+$. Anal. Calcd for $\text{C}_{56}\text{H}_{56}\text{O}_{10}$: C, 75.65; H, 6.35. Found: C, 75.41; H, 6.18.

Acknowledgment. We thank the National Natural Science Foundation of China (20532030, 20625206, 20772126), the National Basic Research Program (2007CB808004), and the Chinese Academy of Sciences for financial support. We also thank Dr. H. B. Song at Nankai University for determining the crystal structures.

Supporting Information Available: Copies of ^1H NMR and ^{13}C NMR spectra for new compounds, ^1H NMR, ^1H – ^1H COSY, and ^1H – ^1H TOCSY spectra of $\mathbf{1} \cdot \mathbf{G2} \cdot 4\mathbf{PF}_6$ at low temperatures, CV curves of $\mathbf{1} \cdot \mathbf{G1} \cdot 2\mathbf{PF}_6$, and X-ray crystallographic files (CIF) for $\mathbf{1} \cdot \mathbf{G1} \cdot 2\mathbf{PF}_6$ and $\mathbf{1} \cdot \mathbf{G2} \cdot 4\mathbf{PF}_6$. This material is available free of charge via the Internet at <http://pubs.acs.org>.

(15) (a) Balzani, V.; Credi, A.; Mattersteig, G.; Matthews, O. A.; Raymo, F. M.; Stoddart, J. F.; Venturi, M.; White, A. J. P.; Williams, D. J. *J. Org. Chem.* **2000**, *65*, 1924–1936. (b) Ikeda, T.; Aprahamian, I.; Stoddart, J. F. *Org. Lett.* **2007**, *9*, 1481–1484.